

## $NN$ Interaction in Chiral Constituent Quark Models

A. Valcarce<sup>1</sup>, F. Fernández<sup>1</sup>, P. González<sup>2</sup>

<sup>1</sup> Grupo de Física Nuclear, Universidad de Salamanca, E-37008 Salamanca, Spain

<sup>2</sup> Dpto. de Física Teórica and IFIC, Universidad de Valencia-CSIC, E-46100 Burjassot, Valencia, Spain

**Abstract.** We review the actual state in the description of the  $NN$  interaction by means of chiral constituent quark models. We present a series of relevant features that are nicely explained within the quark model framework.

### 1 Introduction

At the end of the 70's the potentialities of quark model calculations in low-energy hadron physics were established. In a series of pioneering works, Isgur and Karl [1] performed a quite successful exhaustive study of the baryon spectra and at the same time the short-range repulsion of the nuclear force was qualitatively explained [2]. These ideas encouraged several groups to undertake the ambitious project of trying to understand the  $NN$  interaction in terms of quark degrees of freedom.

Several authors [3, 4, 5] found a quantitative explanation of the  $NN$  short-range repulsion based on dynamical effects induced by the one-gluon exchange (OGE). One would say that there exists no repulsive potential in the naive sense. The color-magnetic OGE interaction likes to have as many symmetric pairs in the color-spin space as possible. Due to the connection of the spin-color space with the orbital space as a consequence of the Pauli principle the orbital symmetry  $[42]_O$  is preferred. But this symmetry has to have a zero in the S-wave. This zero yields for the phase shift the same results as a hard or a soft core.

Based on this success simple quark models of the nuclear force were constructed. The so-called *hybrid quark models* [4] contained three main ingredients: (i) A short range part given by the quark-exchange interaction, (ii) a long range part by the one-pion exchange (OPE) potential, and (iii) a medium range part by a phenomenological potential or a two-pion exchange potential. These meson exchange potentials were considered to simulate the meson cloud sur-

rounding the quark core. These models allowed to reproduce the  $NN$  scattering and bound state data. The next conceptual step in order to understand the  $NN$  interaction only based on quark degrees of freedom was the consideration of  $(q\bar{q})$  and  $(q\bar{q})^2$  excitations generated by off-shell terms of the Fermi-Breit quark-gluon interaction [6]. Although the obtained potential acquired an attractive part in the 0.8–1.5 fm range, it was too weak to bind the deuteron or to fit the extreme low-energy S-wave scattering.

In the middle 80's quark antisymmetry effects on the OPE started to be analyzed [7]. A similar  $NN$  short-range repulsion to the one provided by the OGE was obtained. A first quark-model calculation based on gluon and pion exchange at the level of quarks was performed [8]. As the OPE contributes to the  $\Delta - N$  mass difference, the rather big quark-gluon coupling constant used in the previous models ( $\alpha_s > 1$ ) got nicely reduced to values around 0.5. However, it was not obtained enough intermediate range attraction. To avoid this problem, a phenomenological scalar potential at baryonic level was introduced, returning on this way to a hybrid model. Besides, its coupling constant was fitted to a different value for  $NN$  S-waves, than for higher angular momentum partial waves or for the deuteron [8].

## 2 The Chiral Constituent Quark Model

In the early 90's the constituent quark mass was related to the breaking of chiral symmetry [9, 10]. The underlying idea is that the constituent quark mass is a consequence of the spontaneous chiral symmetry breaking. Then, between the chiral symmetry breaking scale ( $\Lambda_{\text{CSB}} \sim 1$  GeV) and the confinement scale, ( $\Lambda_{\text{C}} \sim 0.2$  GeV) QCD may be simulated in terms of an effective theory of constituent quarks interacting through Goldstone modes. Specifically, in a Nambu-Goldstone realization of chiral symmetry within the linear sigma model, there appear two Goldstone boson fields: the pion and the sigma. The chiral constituent quark model incorporates OPE and one-sigma exchange (OSE) interactions of the form,

$$V_{\text{OPE}}(\mathbf{r}_{ij}) = \frac{1}{3} \alpha_{ch} \frac{\Lambda^2}{\Lambda^2 - m_\pi^2} m_\pi \left\{ \left[ Y(m_\pi r_{ij}) - \frac{\Lambda^3}{m_\pi^3} Y(\Lambda r_{ij}) \right] \boldsymbol{\sigma}_i \cdot \boldsymbol{\sigma}_j + \left[ H(m_\pi r_{ij}) - \frac{\Lambda^3}{m_\pi^3} H(\Lambda r_{ij}) \right] S_{ij} \right\} \boldsymbol{\tau}_i \cdot \boldsymbol{\tau}_j, \quad (1)$$

$$V_{\text{OSE}}(\mathbf{r}_{ij}) = -\alpha_{ch} \frac{4m_q^2}{m_\pi^2} \frac{\Lambda^2}{\Lambda^2 - m_\sigma^2} m_\sigma \left[ Y(m_\sigma r_{ij}) - \frac{\Lambda}{m_\sigma} Y(\Lambda r_{ij}) \right], \quad (2)$$

$\Lambda$  being a cutoff parameter and  $Y(x)$  and  $H(x)$  the standard Yukawa functions. Perturbative features of QCD are incorporated through the OGE potential,

$$V_{\text{OGE}}(\mathbf{r}_{ij}) = \frac{1}{4} \alpha_s \boldsymbol{\lambda}_i \cdot \boldsymbol{\lambda}_j \left\{ \frac{1}{r_{ij}} - \frac{\pi}{m_q^2} \left[ 1 + \frac{2}{3} \boldsymbol{\sigma}_i \cdot \boldsymbol{\sigma}_j \right] \delta(\mathbf{r}_{ij}) - \frac{3}{4m_q^2 r_{ij}^3} S_{ij} \right\}, \quad (3)$$

where the  $\lambda$ 's stand for the color SU(3) matrices. Finally, a phenomenological confining potential is introduced. Its detailed radial structure, being fundamental to study the hadron spectra, is expected to play a minor role for the two-baryon interaction. To be consistent with meson spectroscopy it can be taken to be linear

$$V_{\text{CON}}(\mathbf{r}_{ij}) = -a_c \boldsymbol{\lambda}_i \cdot \boldsymbol{\lambda}_j r_{ij}, \quad (4)$$

though for simplicity harmonic oscillator quark wave functions will be used for the  $NN$  interaction.

This model is able to reproduce quite nicely the  $NN$  scattering and bound state data [10, 11]. Typical values for the parameters are given in Table 1. Other quark-model approaches to the  $NN$  interaction are found in the literature [12].

**Table 1.** Quark-model parameters.

$m_q$ MeV	$b$ fm	$\alpha_s$	$a_c$ MeV fm $^{-1}$	$\alpha_{ch}$	$r_0$ fm	$m_\sigma$ fm $^{-1}$	$m_\pi$ fm $^{-1}$	$\Lambda$ fm $^{-1}$
313	0.518	0.485	67.0	0.0269	0.25	3.42	0.7	4.2

### 3 Several Reasons to Use Quark Models

#### 3.1 Medium Range Attraction

A new feature of the chiral constituent quark model is that through the OSE potential incorporates in a natural way the  $NN$  medium range attraction without any additional parameter. This fact is illustrated in Fig. 1 where we compare the scalar potential obtained at quark level (solid line) with the baryonic parametrization used in ref. [8] (dashed line) to fit the experimental data. While at the baryonic level two different coupling constants are used:  $g_{\sigma NN}^2/4\pi = 3.7$  for (S,T)=(0,1) and  $g_{\sigma NN}^2/4\pi = 1.9$  for (S,T)=(1,1), the quark model result is

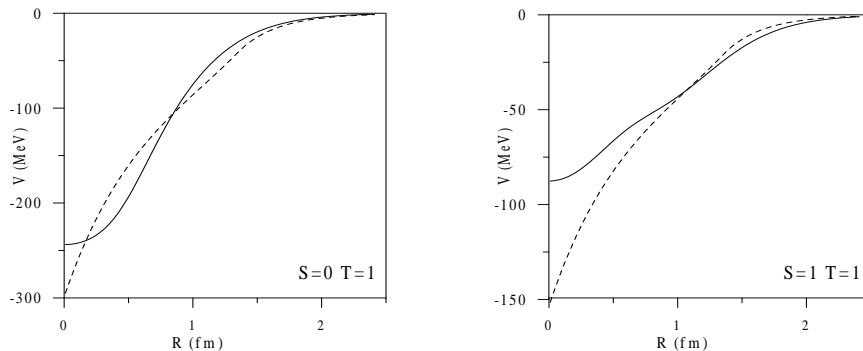


**Figure 1.**  $NN$   $\sigma$  exchange potential

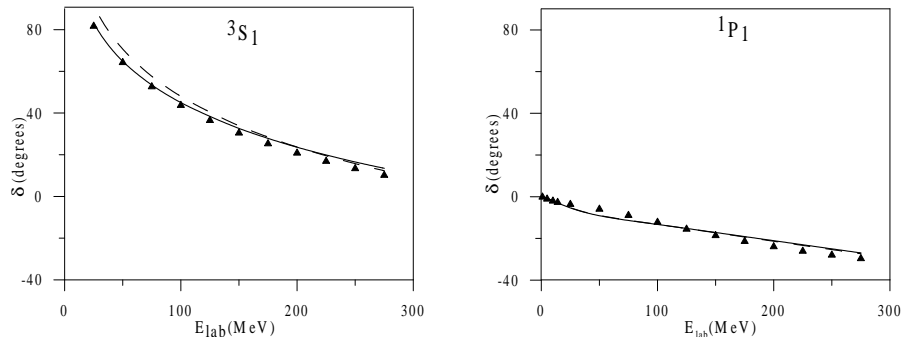


**Figure 2.**  ${}^3S_1$  and  ${}^1P_1$   $NN$  phase shifts

obtained in both cases with the same parameters fixed from the  $\pi qq$  coupling constant. In Fig. 2 we compare the phase shifts for both cases and we can see how the predictions are similar.

### 3.2 $NN$ Short-Range Repulsion

The  $NN$  short-range behavior has been explained in terms of an interplay between quark antisymmetry and a particular quark dynamics. In a group theory language, a completely antisymmetric six quark state asymptotically describing two free nucleons in a relative S-wave is given,

$$\Psi_{NN} = [\Psi_{\{6\}} + \sqrt{8}\Psi_{\{42\}}] / 3, \quad (5)$$

where

$$\begin{aligned} \Psi_{\{6\}} &= [2^3]_C [6]_O [33]_{ST}, \\ \Psi_{\{42\}} &= \frac{1}{\sqrt{2}} [2^3]_C [42]_O ([33]_{ST} - [51]_{ST}), \end{aligned} \quad (6)$$

the subindex C, O or ST indicating the color, orbital or spin-isospin representation respectively. When the distance between the two clusters goes to zero the  $\{42\}$  configuration increases in energy. According to our harmonic oscillator wave function ansatz for the quarks, the excitation energy is given by,

$$\Delta_{ho} \equiv \Delta [E_{\{42\}} - E_{\{6\}}]_{ho} = 2\hbar\omega = \frac{2\hbar^2}{3b^2 m_q}. \quad (7)$$

Let us now consider other interactions. Assume first that quarks interact via the OGE used in ref. [4] ( $\alpha_s = 1.39$ ,  $m_q = 300$  MeV and  $b = 0.6$  fm). We can estimate the energy contribution of the OGE calculating the matrix element,  $\langle \{ \} | \sum_{i < j} V_{OGE}(\mathbf{r}_{ij}) | \{ \} \rangle$  where  $\{ \}$  stands for the  $\Psi_{\{42\}}$  and  $\Psi_{\{6\}}$  configurations of Eq. (6). As we are interested in the  $NN$  interaction energy we should subtract twice the corresponding nucleon self-energy given

by  $\langle N | \sum_{i<j} V_{\text{OGE}}(\mathbf{r}_{ij}) | N \rangle$ . For (S,T)=(1,0), the matrix element of the color magnetic potential for the {6} configuration is 48.83 MeV, while for the {42} configuration is  $-235.63$  MeV. Since in the energy difference between the {42} and {6} configurations the subtracted self-energies cancel, we have  $\Delta_{\text{OGE}} \equiv \Delta [E_{\{42\}} - E_{\{6\}}]_{\text{OGE}} = -284.46$  MeV. This difference compensates the harmonic oscillator energy difference,  $\Delta_{\text{ho}} = 240.36$  MeV, the  $[42]_{\text{O}}$  orbital symmetry becoming the lowest in energy. As a consequence of this configuration mixing the S-wave  $NN$  relative motion wave function shows an energy independent node, which translates into a hard-core behavior in the phase shift.

In the case of the chiral constituent quark model the value of  $\alpha_s$ , which drives the OGE energy gap between the {42} and {6} configurations, is significantly reduced due to the pseudoscalar contribution to the  $\Delta - N$  mass difference and correspondingly the mixing effect. If we recalculate the contribution of the OGE with the parameters of Table 1, we observe again a decrease of the energy difference between the {42} and the {6} configurations  $\Delta_{\text{OGE}} = -140.99$  MeV, but it is much smaller than the harmonic oscillator energy difference  $\Delta_{\text{ho}} = 309.10$  MeV and it is not sufficient to give rise to a significant configuration mixing. It is then convenient to deep in the understanding of the repulsion mechanism.

A similar kind of analysis can be carried out for the OPE and OSE potentials. For (S,T)=(1,0), differently than in the OGE case, the OPE has the same sign for both configurations. Regarding the energy difference one gets  $\Delta_{\text{OPE}} = -68.62$  MeV. Concerning the OSE one has  $\Delta_{\text{OSE}} = 133.05$  MeV. Therefore, in the chiral constituent quark model three effects conspire against the symmetry mixing. First, the small value of  $\alpha_s$ . Second, the cancellation between the OPE contributions to the {42} and {6} configurations, and finally the contrary effect of the OSE potential. Putting all the contributions together one obtains,  $\Delta [E_{\{42\}} - E_{\{6\}}]_{\text{OGE+OPE+OSE}} = -76.56$  MeV, which is much smaller than the harmonic oscillator energy difference  $\Delta_{\text{ho}} = 309.10$  MeV. Then, one must conclude that in the chiral constituent quark model there is not enough configuration mixing to account for the hard-core of the  $NN$  interaction as a node produced by the  $[42]_{\text{O}}$  orbital symmetry.

To look for the origin of this repulsive character of the interaction one should go beyond the energy difference between the symmetries and calculate the specific contribution of the interaction for each symmetry. In order to see the repulsive or attractive character of every term of the potential in both configurations one has to subtract twice the corresponding nucleon self-energy, given by  $\mathcal{E}_{\text{OGE}} = -72.63$  MeV,  $\mathcal{E}_{\text{OPE}} = -311.40$  MeV, and  $\mathcal{E}_{\text{OSE}} = -66.90$  MeV. One then obtains,  $E_{\{6\}}^{\text{OGE+OPE+OSE}} = 455.72$  MeV and  $E_{\{42\}}^{\text{OGE+OPE+OSE}} = 379.16$  MeV. It is then clear that the chiral potential produces strong repulsion in both configurations, {42} and {6}. The OPE hardly contributes to the mixing between them, however in both symmetries it produces strong repulsion. The OGE reduces the energy difference whereas the OSE increases this energy difference and produces an additional attraction in both configurations. The whole effect is an energy difference of about the same

value obtained with the harmonic oscillator model but with an additional repulsion in both symmetries originated mainly by quark antisymmetry on the OPE. Therefore, in this type of models the  $NN$  S-wave behavior should be attributed to the strong repulsion generated by the OPE in the  $[6]_O$  orbital configuration.

### 3.3 Universality

A main feature of the quark treatment is its universality in the sense that all the baryon-baryon interactions are treated on an equal footing. Moreover, once the model parameters are fixed from  $NN$  data there are no free parameters for any other case. This allows a microscopic understanding and connection of the different baryon-baryon interactions that is beyond the scope of any analysis based only on effective hadronic degrees of freedom. We will illustrate our discussion by means of the recently calculated  $NN \rightarrow NN^*(1440)$  transition potential [13]. In particular we will determine the  $\pi NN^*(1440)$  and  $\sigma NN^*(1440)$  coupling constants.

For this purpose, let us realize that asymptotically ( $R \geq 4$  fm) the OSE and OPE potentials have at the baryon level the same spin-isospin structure than at the quark level. Hence we can parametrize the asymptotic central interactions as,

$$V_{NN \rightarrow NN^*(1440)}^{OPE}(R) = \frac{1}{3} \frac{g_{\pi NN}}{\sqrt{4\pi}} \frac{g_{\pi NN^*(1440)}}{\sqrt{4\pi}} \frac{m_\pi}{2M_N} \frac{m_\pi}{2(2M_r)} \frac{\Lambda^2}{\Lambda^2 - m_\pi^2} [(\boldsymbol{\sigma}_N \cdot \boldsymbol{\sigma}_N)(\boldsymbol{\tau}_N \cdot \boldsymbol{\tau}_N)] \frac{e^{-m_\pi R}}{R}, \quad (8)$$

and

$$V_{NN \rightarrow NN^*(1440)}^{OSE}(R) = - \frac{g_{\sigma NN}}{\sqrt{4\pi}} \frac{g_{\sigma NN^*(1440)}}{\sqrt{4\pi}} \frac{\Lambda^2}{\Lambda^2 - m_\sigma^2} \frac{e^{-m_\sigma R}}{R}, \quad (9)$$

where  $g_i$  stands for the coupling constants at the baryon level and  $M_r$  is the reduced mass of the  $NN^*(1440)$  system.

By comparing these baryonic potentials with the asymptotic behavior of the OPE and OSE obtained from the quark calculation we can extract the  $\pi NN^*(1440)$  and  $\sigma NN^*(1440)$  coupling constants in terms of the elementary  $\pi qq$  coupling constant and the one-baryon model dependent structure. The sign obtained for the meson- $NN^*(1440)$  coupling constants comes determined by the arbitrarily chosen relative sign between the  $N$  and  $N^*(1440)$  wave functions. Only the ratios between the  $\pi NN^*(1440)$  and  $\sigma NN^*(1440)$  would be free of this uncertainty.

To get  $g_{\pi NN^*(1440)}/\sqrt{4\pi}$  we turn to our numerical results for the  $^1S_0$  OPE potential, and fit its asymptotic behavior to Eq. (8). We obtain

$$\frac{g_{\pi NN}}{\sqrt{4\pi}} \frac{g_{\pi NN^*(1440)}}{\sqrt{4\pi}} \frac{\Lambda^2}{\Lambda^2 - m_\pi^2} = -3.73, \quad (10)$$

i.e.  $g_{\pi NN^*(1440)}/\sqrt{4\pi} = -0.94$ . As explained above only the absolute value of this coupling constant is well defined. The coupling scheme dependence can be explicitly eliminated if we compare  $g_{\pi NN^*(1440)}$  with  $g_{\pi NN}$  extracted from the  $NN \rightarrow NN$  potential within the same quark model approximation. We get

$$|g_{\pi NN^*(1440)}/g_{\pi NN}| = 0.25. \quad (11)$$

By proceeding in the same way for the scalar potential we can write

$$|g_{\sigma NN^*(1440)}/g_{\sigma NN}| = 0.47. \quad (12)$$

The ratio given in Eq. (11) is similar to that obtained in ref. [14]. Nonetheless one can find values for  $f_{\pi NN^*(1440)}$  ranging between 0.27–0.47 coming from different experimental analyses. Regarding the ratio obtained in Eq. (12), our result agrees quite well with the only experimental available result, obtained in ref. [15] from the fit of the cross section of the isoscalar Roper excitation in  $p(\alpha, \alpha')$  in the 10–15 GeV region, where a value of 0.48 is given. Finally, we can give a very definitive prediction of the magnitude and sign of the ratio of the two ratios,

$$g_{\pi NN^*(1440)}/g_{\pi NN} = 0.53 g_{\sigma NN^*(1440)}/g_{\sigma NN}. \quad (13)$$

### 3.4 Pauli Blocking

The Pauli principle plays an essential role to explain the atomic and nuclear structure. For example, the strong repulsion existing in the  $\alpha\alpha$  system originates from the nucleonic substructure of the  $\alpha$  particle and not from a particular dynamics. The hard-core appears because the saturation of nuclear spin-isospin degrees of freedom allows only four nucleons in the orbital ground state. We shall refer to this saturation phenomenon indicated by the existence of forbidden states at the underlying structure level as *Pauli blocking*. At the level of subnuclear physics the elementary constituents, the quarks, are fermions so a quark Pauli principle is active.

For identical baryons the symmetrization postulate at the baryonic level gives rise to selection rules on the state of the compound system. At the quark level, assuming SU(2) flavor symmetry, this selection rule appears as a particular case of the action of the quark antisymmetrizer,  $\mathcal{A}$ , on a two cluster state from six identical quarks. Taking into account that any two-baryon state (LST) can be decomposed in a symmetric plus an antisymmetric part under the exchange of the baryon quantum numbers, one can write for a definite symmetry (specified by  $f$ )

$$\begin{aligned} \Psi_{B_1 B_2}^{\text{LST}}(\mathbf{R}) &= \frac{\mathcal{A}}{\sqrt{1 + \delta_{B_1 B_2}}} \sqrt{\frac{1}{2}} \left\{ \left[ \Phi_{B_1} \left( 123; -\frac{\mathbf{R}}{2} \right) \Phi_{B_2} \left( 456; \frac{\mathbf{R}}{2} \right) \right]_{\text{LST}} + \right. \\ &\quad \left. + (-1)^f \left[ \Phi_{B_2} \left( 123; -\frac{\mathbf{R}}{2} \right) \Phi_{B_1} \left( 456; \frac{\mathbf{R}}{2} \right) \right]_{\text{LST}} \right\}, \quad (14) \end{aligned}$$

where  $B_1$  and  $B_2$  denote the baryons, and  $-\frac{\mathbf{R}}{2}$ ,  $\frac{\mathbf{R}}{2}$  are the positions of the clusters. The antisymmetrizer can be decomposed as,

$$\mathcal{A} = \frac{1}{2} (1 - 9P_{36})(1 - \mathcal{P}), \quad (15)$$

where  $P_{36}$  exchanges quarks 3 and 6, and  $\mathcal{P}$  exchanges the two clusters. The  $1 - \mathcal{P}$  factor implies  $L + S_1 + S_2 - S + T_1 + T_2 - T + f = \text{odd}$ . For non-identical baryons this relation indicates the symmetry associated to a given set of values of (LST). For identical baryons,  $B_1 = B_2$ ,  $f = \text{even}$  (in order to have a non vanishing wave function) and  $L + S + T = \text{odd}$ , reproducing the well-known selection rule. Certainly the effect of the quark substructure goes beyond the  $(1 - \mathcal{P})$  factor in the antisymmetrizer, being also included through the terms containing  $P_{36}$ . Let us study the effects of these quark exchanges in a system of two non-identical baryons, in particular the  $N\Delta$  system. Assuming the three-quark cluster wave function at position  $\mathbf{S}$  given by

$$\Phi_B(123; \mathbf{S}) = \prod_{i=1}^3 \eta_{0s}(\mathbf{r}_i - \mathbf{S}) \otimes [3]_{\text{ST}} \otimes [1]_{\text{C}}, \quad (16)$$

where  $\eta_{0s}(\mathbf{x})$  is a gaussian with parameter  $b$ , and  $[3]_{\text{ST}}$  ( $[1]_{\text{C}}$ ) stands for the spin-isospin (color) representation, the norm of the projected  $\Psi_{N\Delta}^{\text{LST}}$  state reads,

$$N_{N\Delta}^{\text{LST}}(R) = N_L^{\text{di}}(R) - C(S, T, f) N_L^{\text{ex}}(R), \quad (17)$$

where  $N_L^{\text{di}}(R)$  [ $N_L^{\text{ex}}(R)$ ] refers to the direct [exchange] radial contribution coming from the  $1[P_{36}]$  term in the antisymmetrizer. The spin-isospin coefficient  $C(S, T, f)$  is given by,

$$C(S, T, f) = 3 \left\{ {}_{\text{ST}} \langle N(123) \Delta(456) | P_{36}^{ST} | N(123) \Delta(456) \rangle_{\text{ST}} + (-1)^f {}_{\text{ST}} \langle N(123) \Delta(456) | P_{36}^{ST} | \Delta(123) N(456) \rangle_{\text{ST}} \right\}. \quad (18)$$

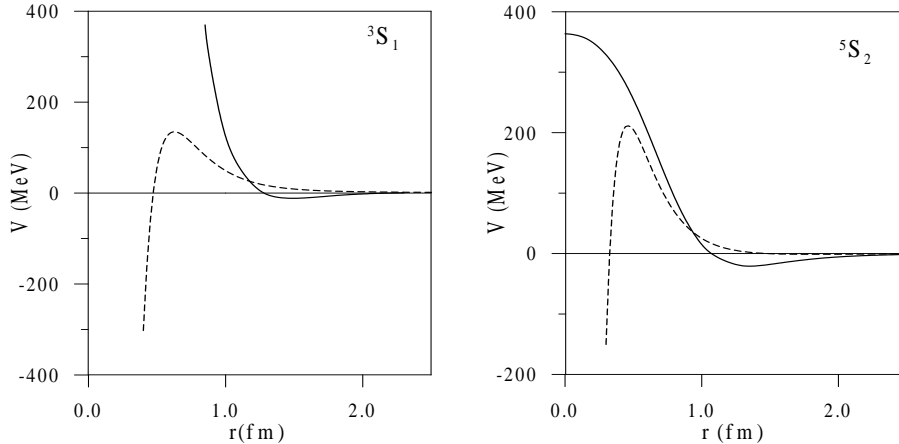


**Figure 3.**  ${}^3S_1(T=1)$  and  ${}^5S_2(T=1)$   $N\Delta$  potentials



Its value for the  $N\Delta$   $S$ -waves is given in Table 2 (the  $NN$  case is also shown for comparison). In the  $R \rightarrow 0$  limit and to the dominant order Eq. (17) transforms

**Table 2.**  $C(S, T, f)$  coefficients for the  $NN$  and  $N\Delta$   $S$ -waves.

	$NN$		$N\Delta$			
	$^1S_0$ ( $T = 1$ )	$^3S_1$ ( $T = 0$ )	$^3S_1$ ( $T = 1$ )	$^3S_1$ ( $T = 2$ )	$^5S_2$ ( $T = 1$ )	$^5S_2$ ( $T = 2$ )
$C(S, T, f)$	$-1/9$	$-1/9$	1	$1/9$	$1/9$	1

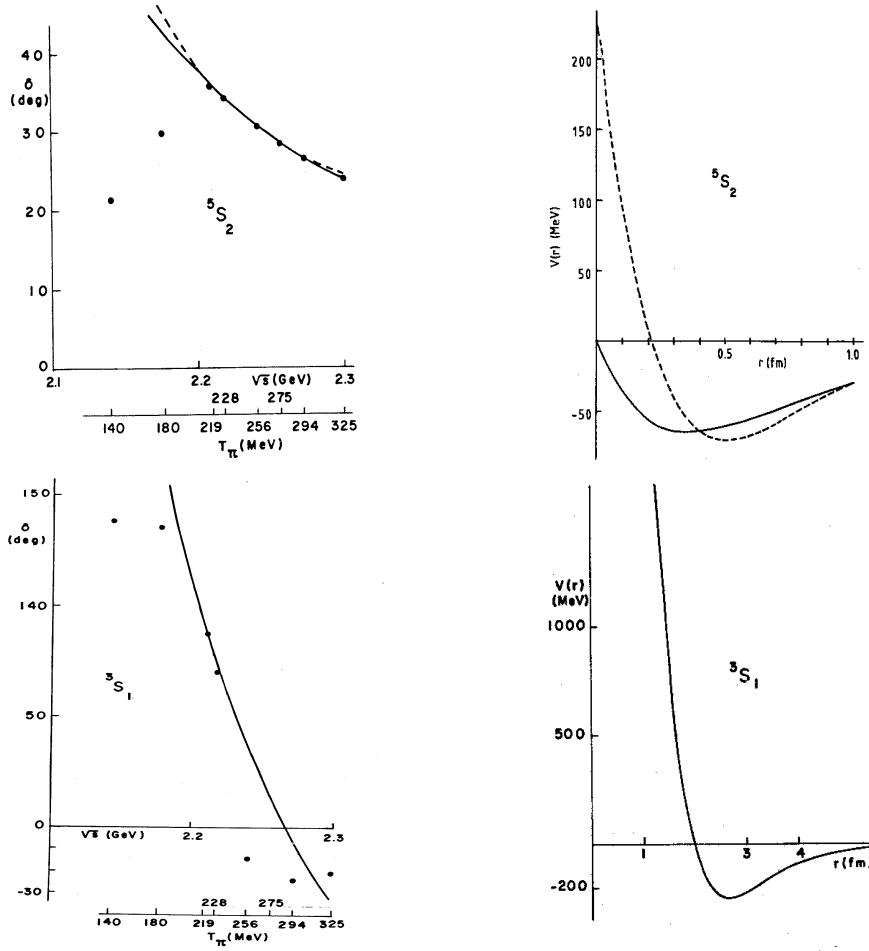


**Figure 4.**  $^3S_1(T = 1)$  and  $^5S_2(T = 1)$   $N\Delta$  phase shifts and separable potential

into:

$$N_{N\Delta}^{\text{LST}}(R) \xrightarrow{R \rightarrow 0} 4\pi \left[ 1 - \frac{3R^2}{4b^2} \right] \frac{1}{1 \cdot 3 \cdots (2L+1)} \left[ \frac{R^2}{4b^2} \right]^L \times \left\{ [3^L - C(S, T, f)] + \frac{1}{2(2L+3)} \left[ \frac{R^2}{4b^2} \right]^2 [3^{L+2} - C(S, T, f)] + \cdots \right\} \quad (19)$$

Then, for  $3^L = C(S, T, f)$  the overlapping of the two-cluster wave function behaves as  $R^{2L+4}$  instead of the centrifugal barrier behavior  $R^{2L}$ , indicating that quark Pauli blocking occurs (in other words, a node appears in the relative wave function). This turns out to be the case (see Table 2) for the  $N\Delta$  partial waves  ${}^3S_1(T=1)$  and  ${}^5S_2(T=2)$  giving rise to forbidden states (the  $[6]_{\text{O}}$  orbital configuration for  $L=0$ ). If we now calculate the  $N\Delta$  potential, we observe (solid line) the important difference between the potential in a Pauli blocked and a non Pauli blocked channel (see Fig. 3). At the same time we have represented by the dashed line a  $N\Delta$  potential obtained from a direct scaling of the  $NN$  interaction [16] and we see how the difference between the two channels is just a spin-isospin factor. As shown in Fig. 4, a separable  $N\Delta$  potential reproducing the phase shifts obtained from the experimental  $\pi d$  elastic cross section presents the strong repulsion predicted by the quark model in the  ${}^3S_1(T=1)$  partial wave [17].

A similar analysis for the  $NN$  system does not show any forbidden configuration, see Table 2. As we have seen, the  $NN$  short-range repulsion in the S-waves involves dynamical effects.

### 3.5 Connection to Other Systems: The Baryon Spectrum

The chiral constituent quark model allows also to study the baryon spectrum in a completely parameter-free way. We have calculated the nonstrange baryon spectrum within a Faddeev approach. We included all the configurations  $(\ell, \lambda, s, t)$  ( $\ell$  is the orbital angular momentum of a pair,  $\lambda$  is the orbital angular momentum between the pair and the third particle, while  $s$  and  $t$  are the spin and isospin of the pair) with  $\ell$  and  $\lambda$  up to 5.

For this purpose, the delta function of the OGE interaction has to be regularized. By choosing an exponential regularization

$$\delta(\mathbf{r}_{ij}) \Rightarrow \frac{1}{4\pi r_0^2} \frac{e^{-r_{ij}/r_0}}{r_{ij}}, \quad (20)$$

with  $r_0 = 0.25$  fm (a typical value for spectroscopic models) we obtain the  $N$  and  $\Delta$  spectra shown in Fig. 5. The predicted spectrum is reasonable except for the fact that all the negative parity states are around 100 MeV below the experimental data. The relative position of the  $N(1440)$  and the  $N(1535)$  is not very much affected by the modification of  $\alpha_s$  (see Fig. 3 of ref. [18]), indicating that the correct level ordering is not connected with the strength of OGE.

A possible mechanism responsible for the inversion of these states can be obtained through the pseudoscalar interaction. To illustrate this point we have

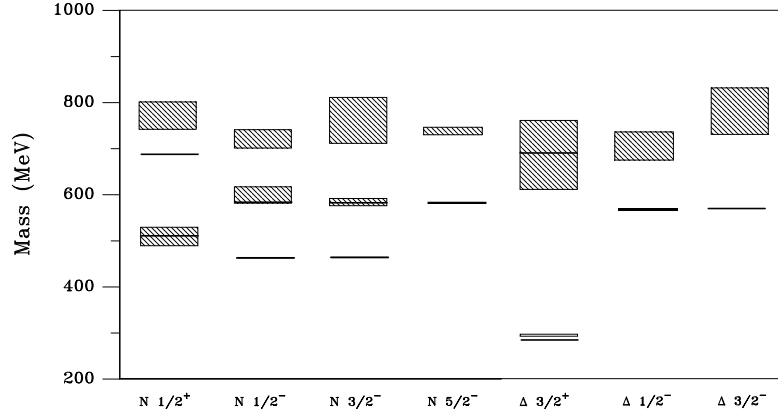


**Figure 5.** Relative energy nucleon and  $\Delta$  spectra

calculated the energy of the  $N(1440)$  and  $N(1535)$  increasing the contribution of the pseudoscalar interaction by letting the cutoff parameter  $\Lambda_\pi$  of the OPE to increase. The results are shown in Fig. 6. As can be seen, the inversion of the ordering between the positive and negative parity states can be achieved if  $\Lambda_\pi$  becomes sufficiently large (around  $7 \text{ fm}^{-1}$  for the set of parameters of Table 2). Such a model would be incompatible with the understanding of the basic features of the two-nucleon system [19].

#### 4 Summary

In this work we have emphasized several physical aspects of the  $NN$  interaction that support the results obtained within the chiral constituent quark model. In particular, medium range attraction is satisfactorily explained and the  $NN$  short-range repulsion is understood through antisymmetry effects on the OPE interaction. Actually, antisymmetry effects at the level of Goldstone bosons appear as a basic tool to understand the  $NN$  phase shifts. Extension of

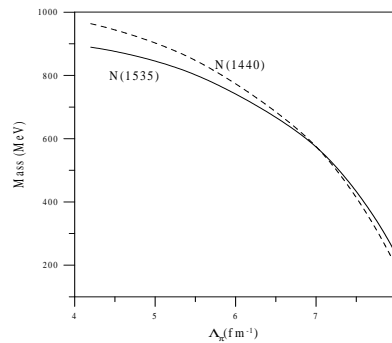


**Figure 6.**  $N(1440)$  and  $N(1535)$  masses as a function of  $\Lambda_\pi$

the model to the general baryon-baryon case is straightforward and parameter-free. From it, non-strange meson-baryon-baryon coupling constants can be calculated. Pauli blocking effects manifest in different partial waves of several systems and find support in indirect experimental data. Such strong repulsion cannot be understood in a meson-exchange model.

Finally, the chiral constituent quark model is able to generate a quite reasonable description of the baryon spectrum with a set of parameters that allows to understand the  $NN$  phenomenology. Therefore, the validity of a model where the OGE is combined with Goldstone-boson exchanges is out of question, and it presents advantages with respect to models based only on Goldstone-boson exchanges, as has been recently emphasized in several works [19, 20].

*Acknowledgement.* This work has been partially funded by Ministerio de Ciencia y Tecnología under Contract No. BFM2001-3563, by Junta de Castilla y León under Contract No. SA-109/01, and by the European Commission IHP program under Contract No. HPRN-CT-2000-00130.

## References

1. N. Isgur, G. Karl: Phys. Rev. **D18**, 4187 (1978)
2. V.G. Neudatchin et al.: Prog. Theor. Phys. **58**, 1072 (1977)
3. H. Toki: Z. Phys. **A294**, 173 (1980)
4. M. Oka et al.: Phys. Lett. **90B**, 41 (1980); Nucl. Phys. **A402**, 477 (1983)
5. A. Faessler et al.: Phys. Lett. **112B**, 201 (1982)
6. Y. Fujiwara, K.T. Hetch: Phys. Lett. **171B**, 17 (1986)
7. K. Shimizu: Phys. Lett. **148B**, 418 (1984)
8. K. Bräuer et al.: Z. Phys. **A320**, 609 (1985) ; Nucl. Phys. **A507**, 599 (1990)
9. I.T. Obukhovskiy, A.M. Kusainov: Phys. Lett. **238B**, 142 (1990)
10. F. Fernández et al.: J. Phys. **G19**, 2013 (1993)
11. A. Valcarce et al.: Phys. Rev. **C50**, 2246 (1994)
12. H.R. Pang et al.: Phys. Rev. **C65**, 014003 (2002)
13. B. Juliá-Díaz et al.: Phys. Rev. **C66**, 024005 (2002)
14. D.O. Riska, G.E. Brown: Nucl. Phys. **A679**, 577 (2001)
15. S. Hirenzaki et al.: Phys. Lett. **B378**, 29 (1996)
16. M.T. Peña et al.: Phys. Rev. **C42**, 855 (1990)
17. E. Ferreira et al.: Phys. Rev. **C36**, 1916 (1987)

18. H. Garcilazo et al.: Phys. Rev. **C64**, 058201 (2001)
19. C. Nakamoto, H. Toki: Prog. Theor. Phys. **99**, 1001 (1998)
20. N. Isgur: Phys. Rev. **D62**, 054026 (2000)

